INLET CROSS-SECTIONAL AREA CALCULATED BY PROCESS-BASED MODEL

Nicholas C. Kraus[1]

ABSTRACT: This paper introduces a process-based model for calculating the equilibrium cross-sectional area of a tidal inlet and temporal behavior of small perturbations in channel area from equilibrium. The model accounts for the dynamic balance between inlet ebb-tidal transport and longshore sand transport at the inlet entrance. Expressed in terms of a water discharge through the inlet and the gross longshore sand transport rate, the formulation can account for tidal, river, and wind-driven flows. The resultant predictive equation recovers the form of the well-known empirical formula $A_E = CP^n$, where A_E is the equilibrium (minimum) cross-sectional area, P is the tidal prism, and C and n are empirical coeffieients. An explicit expression is obtained for C in terms of coastal sediment-transport processes, and the value of n derived is in the range found empirically. The process-based model qualitatively predicts the difference in trends in inlet cross-sectional area on wave-sheltered and fully-exposed coasts. In time-dependent mode, the model reproduces qualitative behavior of the departure of the cross-sectional area from equilibrium under perturbations in the driving forces of discharge and waves.

INTRODUCTION

A quantitative empirical relation between the equilibrium or minimum stable cross-sectional area A_E of an inlet and its tidal prism P has been known for almost a century (LeConte 1905). Based on data from a limited number of locations along the coast of California, LeConte arrived at the linear equation $A_E = CP$. The value of the empirical coefficient C was about 34 % larger for inner harbor entrances (restricted longshore sediment transport) than for unprotected entrances (unrestricted longshore transport). LeConte's observation indicates that the same tidal prism on a coast with restricted longshore transport can maintain a larger equilibrium channel area than on a coast with less restricted or greater longshore sediment transport.

The presently accepted empirical relation for the cross-sectional area of inlets on exposed coasts is still expressed in terms of the bulk properties of the hydrodynamics

1) U.S. Army Engineer Waterways Experiment Station, Coastal and Hydraulics Laboratory, 3909 Halls Ferry Road, Vicksburg, MS 39180-6199 USA. n.kraus@cerc.wes.army.mil.

(tidal prism). Following the work of O'Brien (1931, 1969), Johnson (1972), and others, Jarrett (1976) analyzed 108 inlets (yielding 162 data points) along the Atlantic, Gulf, and Pacific Ocean coasts of the United States. His objectives were to determine if inlets on all three coasts of the United States follow the same inlet area – tidal prism relation, and if inlet stabilization altered that relation. With relatively high correlation coefficients, all predictive relations were found to fit the form

$$A_E = CP^n \tag{1}$$

in which C and n are empirically determined. Jarrett found the exponent n to vary between 0.86 and 1.10 for inlets with no jetty or with a single jetty and between 0.85 and 0.95 for inlets with two jetties. For coasts fully exposed to wave action, n varied between 0.85 and 0.95.

Table 1 summarizes Jarrett's findings (converting his U.S. customary units to metric units). Among other observations, Jarrett (1976) noted that the smaller waves on the Gulf coast relative to those on the Pacific Coast and on (most of) the Atlantic Coast would produce smaller littoral drift.

Table 1. Inlet-area and tidal prism regression values found by Jarrett (1976) for $A_E = CP^n$ (area units of m^2; tidal inlets on U.S. coasts)

	All Inlets		Unjettied, Single-Jettied		Dual Jettied	
Location	C	n	C	n	C	n
All Inlets	1.576×10^{-4}	0.95	3.797×10^{-5}	1.03	7.490×10^{-4}	0.86
Atlantic Coast	3.039×10^{-5}	1.05	2.261×10^{-5}	1.07	1.584×10^{-4}	0.95
Gulf Coast	9.311×10^{-4}	0.84	6.992×10^{-4}	0.86	Insuff. Data	Insuff. data
Pacific Coast	2.833×10^{-4}	0.91	8.950×10^{-6}	1.10	1.015×10^{-3}	0.85

The concept that the equilibrium area of an inlet (tidal entrance or river mouth) is determined by a balance between the transporting capacity of the inlet flow and the littoral or longshore transport has appeared throughout the literature (e.g., LeConte 1905, O'Brien 1931, 1969, Bruun and Gerritsen 1960, Bruun 1968, Byrne et al. 1980, Riedel and Gourlay 1980, Hume and Herdendorf 1990). In particular, Byrne et al., Riedel and Gourlay, and Hume and Herdendorf studied inlet channel stability on sheltered coasts and demonstrated that larger values of the empirical coefficient C and smaller values of n apply to coasts with limited littoral transport. Quoting Riedel and Gourlay, "In contrast (to exposed coasts), for sheltered inlets the littoral drift rate is small and, consequently, a much smaller volume of material needs to be moved out of the entrance in each tidal cycle." The aforementioned three studies also indicate that the mean-maximum velocity (mean over the cross section of the maximum at spring tide; see Bruun (1978), p. 321) required to maintain stability of the inlet channel is less (reaching approximately one-third less) than the typical 1 m/s (Bruun and Gerritsen 1960, O'Brien 1969) required to maintain a channel on an exposed coast.

Changes in inlet cross-sectional channel in response to changes in hydrodynamic forcing (waves, tidal or river current, tidal range. storms) have been documented by Mason and Sorensen (1972), Byrne et al. (1974), Behrens et al. (1977), FitzGerald and FitzGerald (1977), Nummedal and Humphries (1978), Van de Kreeke and Haring (1980), and others. FitzGerald and FitzGerald also discuss inlet channel response to changes in neighboring beach morphology.

In this paper, a mathematical model is introduced that describes, in a rational and quantitative way, the two main concepts described above. First, the model produces an equilibrium or stable channel cross section under the balance of tidal (and river) transporting capacity and the longshore sediment transport at the inlet. Second, the model can describe variations of the cross-section about its equilibrium in response to small changes in sediment-transport forces. The time scale governing the response of a channel to perturbations is also obtained.

PROCESS-BASED APPROACH

In the following, a tidal-inlet entrance or river mouth is considered on an alluvial shore with no geologic controls such as a rock or clay substratum.

Referring to Fig. 1, we assume that an ebb shoal or entrance bar forms and is maintained by a balance between the transport capacities of the ebb-tidal (or river) current and the longshore current. The gross longshore transport rate Q_g is given by

$$Q_g = \varepsilon_L Q_L + \varepsilon_R Q_R \tag{2}$$

where ε_L and ε_R are efficiency factors associated with the longshore transport rates for sediment moving to the left (for an observer on land) at rate Q_L and to the right at rate Q_R. The cfficiency factors are, in general, functions of time and vary between the limits $0 \leq \varepsilon \leq 1$ to account for blocking at jetties, bar bypassing, sediment availability, and similar processes. In this paper, $\varepsilon = 1$.

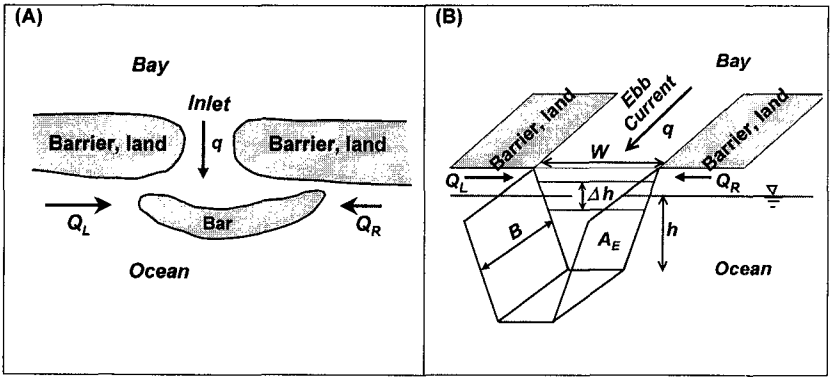

Fig. 1. Definition sketch for process model, (A) plan view, and (B) cross-section view.

The rate of sediment transport out of the inlet entrance is qW. Here q is the rate per unit width (m^3/s per meter across the inlet channel) as transported by the current (whether tidal-ebb, river-, or wind-generated current, or a combination), and W is the width of the inlet. We are interested in the channel equilibrium area, related to the water volume above the sea bottom. The time rate of change in bulk volume of sediment transported to the channel V_S and that of the volume of water V above the bed are related as $dV_S/dt = -dV/dt$, where t is time. Balance of the rates of sediment transported to the channel bar in Fig. 1 with the change in volume of water above the channel gives

$$\frac{dV}{dt} = qW - Q_g \tag{3}$$

If simple rectangular geometry for the entrance bar is assumed such that the $V = BWh$, where B and h are, respectively, the cross-shore width of and depth over the bar, and further assuming B is constant, then the channel area $A = Wh$, and Eq. 3 becomes

$$\frac{dA}{dt} = \frac{W}{B}q - \frac{1}{B}Q_g \tag{4}$$

The gross longshore sediment transport rate Q_g will be assumed to be known, as from the CERC formula or data. The transport rate q will be expressed as a Meyer-Peter and Muller (power law) in the form expressed by Watanabe et al. (1991) as

$$q = \alpha \frac{(\tau_m - \tau_c)}{\rho g} v_m \tag{5}$$

in which α is an empirical coefficient expected to be of order unity, τ_m is the bottom shear stress associated with the mean maximum velocity, τ_c is the critical shear stress for sediment transport, ρ is the fluid density, g is the acceleration of gravity, and v_m is the depth-averaged mean-maximum velocity along the channel. In the following, τ_c will be neglected. The critical shear could play a role at inlets where the hydrodynamic forces are weak or at inlets with coarse sediments.

The bottom shear stress under the maximum current is parameterized as

$$\tau_m = \rho c_f v_m^2 \tag{6}$$

where c_f is a bottom friction coefficient taken to be $c_f = gm^2/h^{1/3}$ where m^2 is the Mannings coefficient squared (units of $s^2/m^{2/3}$). Then Eq. 5 becomes,

$$q = \frac{\alpha m^2}{h^{1/3}} v_m^3 \tag{7}$$

and Eq. 4 becomes

$$\frac{dA}{dt} = \frac{\alpha m^2 W}{B h^{1/3}} \left(\frac{D_m}{A} \right)^3 - \frac{1}{P} Q_g \tag{8}$$

in which the velocity was replaced by $v_m = D_m/A$, where D_m is the maximum discharge, for example, the mean-maximum discharge at spring tide for the case of a tidal inlet without river flow or other non-tidal contribution to the discharge.

At equilibrium, $dA/dt = 0$, giving the equilibrium or minimum channel cross-sectional area A_E as

$$A_E = \Lambda_h D_m \tag{9}$$

where

$$\Lambda_h = \left(\frac{\alpha m^2 W_E}{h_E^{1/3} Q_g} \right)^{1/3} \tag{10}$$

in which h_E and W_E are the depth and width corresponding to the equilibrium area A_E. It is noted that a linear form as Eq. 9 will result for any transport rate formula for q that is a simple algebraic function of v_m or D_m.

Eq. 9 has the same form as the classical Eq. 1, but with the tidal prism P replaced by the discharge D. At equilibrium we have $h_E = A_E/W_E$, where W_E is the width of the channel at equilibrium. Replacing h_E in Eq. 10 by this relation results in

$$A_E = \Lambda D_m^{0.9} \tag{11}$$

where

$$\Lambda = \left(\frac{\alpha m^2 W_E^{4/3}}{Q_g} \right)^{0.3} \tag{12}$$

Eqs. 11 and 12 can be compared to Eq. 1 by assuming that the discharge is solely related to the tidal prism. Keulegan and Hall (1950) assumed a sinusoidal discharge so that the tidal prism P or volume of water ebbing in half a tidal period T is

$$P = \int_0^{T/2} D_m \sin\left(\frac{2\pi}{T} t \right) dt \tag{13}$$

They introduced a coefficient C_K such that $0.81 \leq C_K \leq 1$ to account for a more realistic non-sinusoidal tide, giving,

$$D_m = \frac{\pi C_k}{T} P \tag{14}$$

Then, Eq. 11 expressed in terms of the tidal prism becomes,

$$A_E = C_p P^{0.9} \tag{15}$$

in which the process-based coefficient C_p is given by

$$C_p = \left(\frac{\alpha \pi^3 C_K^3 m^2 W_E^{4/3}}{Q_g T^3} \right)^{0.3} \tag{16}$$

Eq. 15 is similar to the classical and well-verified Eq. 1 with the empirical coefficient C in Eq. 1 replaced by C_p. Eq. 16 shows that C_p depends on Q_g inversely as the 3/10 power, an inverse dependence in qualitative accord with observations for sheltered and unsheltered coasts. The inverse dependence on the tidal period as $T^{0.9}$ is testable if adequate data are available for coasts with a diurnal tide.

Bruun (1978), in his Table 5.35, lists data for 11 jettied and unjettied inlets that include the channel cross-section (assumed to be near equilibrium), maximum discharge, and the approximate total longshore sediment transport to the inlet. The data set contains estimates of annual Q_g ranging from 7×10^4 m^3 (with D_m of 0.87×10^3 m^3/s) for Mission Bay, California to 8×10^5 m^3 (with D_m of 36.4×10^3 m^3/s) for Grays Harbor Washington. In this limited data set, Grays Harbor falls along trend lines to be discussed, but is omitted because the discharge is an order of magnitude larger than any other. The next largest inlet is Thyboron, Denmark, with annual Q_g of 7×10^5 m^3 and D_m of 5.6×10^3 m^3/s.

Figure 2 plots the channel cross-sectional area against the mean-maximum discharge, indicating a close relation, as noted earlier by Bruun and Gerritsen (1968). Figure 3 plots A versus the functional relation $D_m^{0.9}/Q_g^{0.3}$. The scatter about the best-fit line is considerably greater than in Fig. 2 owing, in part, to the uneertainty in knowledge of Q_g. Although the data set is limited, the result is promising. The process-based approach appears capable of predicting the cross-sectional area without necessity of determining an empirical coefficient, while accounting for variations in sediment type (through α and m^2, longshore transport rate, and width of the inlet).

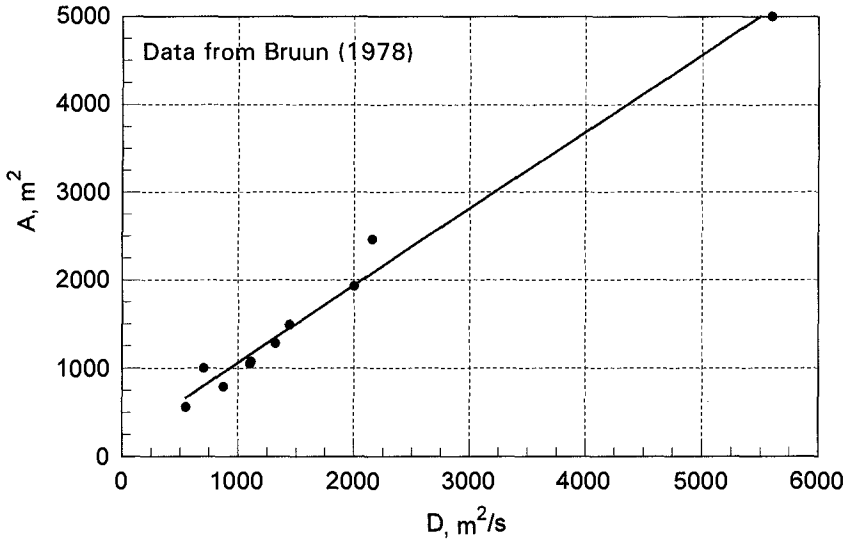

Fig. 2. Inlet cross-sectional area versus discharge.

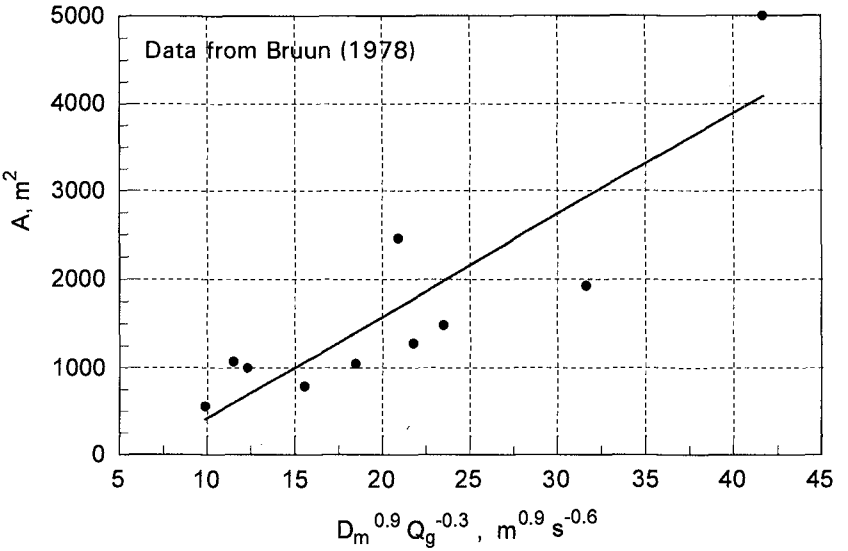

Fig. 3. Inlet cross-sectional area versus functional form of Eq. 11.

To examine the validity of the above formulation, the magnitude of C_p is estimated with representative values for the East Coast of the United States as follows: $\alpha = 1$; $C_K = 1$; $m^2 = (0.025)^2$ s^2/m$^{2/3}$; $W_E = 400$ m; $Q_g = 315{,}000$ m^3/year = 1×10^{-2} m^3/s; and $T = 44{,}712$ s for a semi-diurnal tide. With these values, one finds $C_p \cong 8.7\times10^{-4}$ m$^{-7/10}$. Because of the assumption of constant width of the inlet channel, comparison with C-values for dual-jettied inlets is most appropriate. From Table 1, Jarrett (1976) found $C = 7.5\times10^{-4}$ for all U.S. tidal inlets considered that had dual jetties, and with exponent $n = 0.86$. The close agreement of the estimated C_p and C, as well as the n-values (0.9 derived versus 0.86 empirical) is considered fortuitous, but achieving the correct order of magnitude is encouraging. The exponent 0.3 in Eq. 16 makes the magnitude of C_p relatively insensitive to reasonable changes in values comprising it. For example, changing the value of α from 1 to 0.1 reduces the value of C_p by one-half.

CHANNEL RESPONSE TO TIME-DEPENDENT FORCING

This section explores time dependencies of the change in channel cross-sectional area in the process-based approach.

Characteristic relaxation time

Eq. 8 is the time-dependent governing equation for the channel cross-sectional area $A(t)$. Noting from Eqs. 9 and 10 that

$$A_E^3 = \frac{\alpha\, m^2 W_E}{h_E^{1/3} Q_g} D_m^3 \tag{17}$$

then, assuming that $W_E/h_E^{1/3} = W/h^{1/3}$, Eq. 8 can be rewritten as

$$\frac{dA}{dt} = \frac{Q_g}{B}\left(\frac{A_E^3}{A^3} - 1\right) \tag{18}$$

If, instead, the assumption $W = W_E$ is made, the exponent 3 in Eq. 18 becomes 10/3.

Suppose that for some reason A is perturbed by a certain small amount a from equilibrium, that is, $A(t) = A_E + a(t)$, where $|a|/A_E << 1$, with the driving forces remaining constant. Then, by applying the binomial expansion to lowest order, Eq. 18 becomes

$$\frac{da}{dt} - \frac{1}{\tau_0} a = 0 \tag{19}$$

where $\tau_0 = BA_E/3Q_g$ is a characteristic relaxation time scale for the channel cross section to return to equilibrium according to the solution of Eq. 19, $a = a_0 \exp(-t/\tau_0)$, in which a_o is the magnitude of the initial perturbation. Order-of-magnitude estimates show τ_0 in the approximate range of 0.3 to 2 year.

Time-Varying Forcing

More generally, suppose that the discharge and gross longshore sediment transport rate are time varying, leading to a time variation in the channel cross-section. Let

$$\begin{aligned} A &= A_E + a(t) \\ D &= D_E + d(t) \\ Q_g &= Q_{gE} + Q(t) \end{aligned} \tag{20}$$

where a, d, and Q are small departures from their respective equilibrium values such that $|a|/A_E << 1$, $|d|/D_E << 1$, and $|Q|/Q_{gE} << 1$. Then Eq. 8 becomes

$$\frac{da(t)}{dt} + \frac{\beta}{A_E} a(t) = \frac{\beta}{D_E} d(t) + \frac{1}{B} Q(t) \tag{21}$$

where $\beta = 3Q_{gE}/B$, and

$$\frac{\beta}{A_E} = \frac{3Q_{gE}}{A_E} = \frac{1}{\tau_0} \equiv \sigma_0 \tag{22}$$

This equation is general, subject to the small-perturbation assumption, and can be solved once the functional dependencies of $d(t)$ and $Q(t)$ are known.

As an illustrative analytical solution of Eq. 21, we consider simple sinusoidal forcing, namely,

$$d(t) = d_o \sin(\sigma_1 t)$$
$$Q(t) = Q_o \sin(\sigma_2 t - \phi) \tag{23}$$

where d_o and Q_o are the magnitudes of the perturbations, σ_1 and σ_2 are angular frequencies for the respective perturbations or forcings, and ϕ expresses a possible phase shift between the forcings. For example, σ_1 might relate to a cycle of higher spring tides and corresponding change in the discharge, and σ_2 might relate to seasonal changes in waves. With the notation, $A_1 = \beta\, d_o / D_E$, and $A_2 = Q_o / B$, Eq. 21 becomes

$$\frac{da}{dt} + \sigma_0 a = R(t) \tag{24a}$$

where $R(t)$ is the known forcing,

$$R(t) = A_1 \sin(\sigma_1 t) + A_2 \sin(\sigma_2 t - \phi) \tag{24b}$$

The solution of Eq. 24a for the initial condition $a = 0$ at $t = 0$ is

$$\begin{aligned} a(t) = {} & \frac{\sigma_1 A_1}{\sigma_o^2 + \sigma_1^2}\left(\frac{\sigma_o}{\sigma_1}\sin(\sigma_1 t) - \cos(\sigma_1 t)\right) \\ & + \frac{\sigma_2 A_2}{\sigma_o^2 + \sigma_2^2}\left(\frac{\sigma_o}{\sigma_2}\sin(\sigma_2 t - \phi) - \cos(\sigma_2 t - \phi)\right) \\ & + \left[\frac{\sigma_1 A_1}{\sigma_o^2 + \sigma_1^2} + \frac{\sigma_2 A_2}{\sigma_o^2 + \sigma_2^2}\left(\frac{\sigma_o}{\sigma_2}\sin(\phi) - \cos(\phi)\right)\right]\exp(-\sigma_o t) \end{aligned} \tag{25}$$

Similarly, a numerical solution of Eq. 24a can be developed with the discretization scheme

$$\frac{a' - a}{\Delta t} + \frac{\sigma_0}{2}(a' + a) \approx R(t) \tag{26}$$

where the prime symbol denotes the next time step. Eq. 26 leads to the algorithm

$$a' = \frac{1 - \delta}{1 + \delta} a + \frac{\Delta t}{1 + \delta} R(t) \tag{27}$$

in which $\delta = \sigma_0 \Delta t / 2$. Solutions with Eq. 27 will be plotted for comparison with the analytic solution given by Eq. 25. Eq. 27, which is unconditionally stable, is a general numerical solution to Eq. 24 for any given forcing $R(t)$ and associated initial condition.

Eqs. 25 and 27 were calculated with the values given in Table 2. The parameter values correspond to a moderately-sized inlet on the east coast of the United States with $A_E \cong 10^3$ m^2, $Q_{gE} \cong 3\times10^5$ m^3/year, and $B \cong 3\times10^2$ m. The annual maximum of spring tides, hence greatest mean-maximum discharge, was assumed to have periodicity of a half-year, and the gross longshore sand transport rate was given an annual cycle to represent a characteristic winter-summer difference in wave conditions.

Table 2. Values of parameters for the sinusoidal forcing perturbation example.

A_1 m^2/year	A_2 m^2/year	$\lvert d_0\rvert/D_E$	$\lvert Q\rvert/Q_{gE}$	σ_0 day^{-1}	σ_1 day^{-1}	σ_2 day^{-1}
100	100	1/10	1/10	1/120	$2\pi/182.5$	$2\pi/365$

Calculations for an elapsed time of 3 years after initiation of the perturbative forcing are plotted in Figs. (4) and (5) for phase lags ϕ of 0 and π, respectively. Both the analytical and numerical solutions are shown in these figures. For the numerical solution, the forcing $R(t)$ was set to 0 after 1.5 years to show the decay of the perturbation (dashed line) according to the relaxation time τ_0. The time step for the calculation was Δt = 1 day. Even for this relatively large time step, the analytical and numerical solutions are almost indistinguishable (prior to setting of the forcing to zero).

The transient portion of the solution for this example damps after about one-half year. After that, the perturbation a varies periodically. Phasing between the two forcings of discharge and longshore transport rate can greatly alter the behavior of the solution at initiation of the forcing or for a change in forcing. In the present example, the two lags produced a difference in cross-sectional area of approximately 45 m^2 in the first half year (difference of +23 m^2 and -22 m^2).

As a final example, a calculation was made with parameters held as in Table 2, except that σ_1 was changed to an approximate fortnightly variation. Also, Δt was reduced to 0.5 day to allow the numerical solution to better capture the rapid variations in the inlet cross-sectional response, as shown in Fig. 6. The more rapid variation in the discharge, as compared to that shown in Figs. 4 and 5, produces considerably smaller changes in the cross-sectional area. The inertia of the inlet system does not allow rapid response of the cross-section, being scaled by the relaxation time τ_0. In addition, because one of the two forcings does not have sufficient time to fully develop, the magnitude of the total response is less than shown in the previous example, where the periods of the forcings were longer and comparable.

In summary, on the assumption that a channel cross section tends to be stable, Eq. 21 is capable of describing small changes in area about equilibrium in response to changes in the two major forcings that move sediment along or toward the channel. Such changes have been documented by Byrne et al. (1974), Behrens et al. (1977), FitzGerald and FitzGerald (1977), Nummedal and Humphries (1978), Van de Kreeke and Haring (1980), and others.

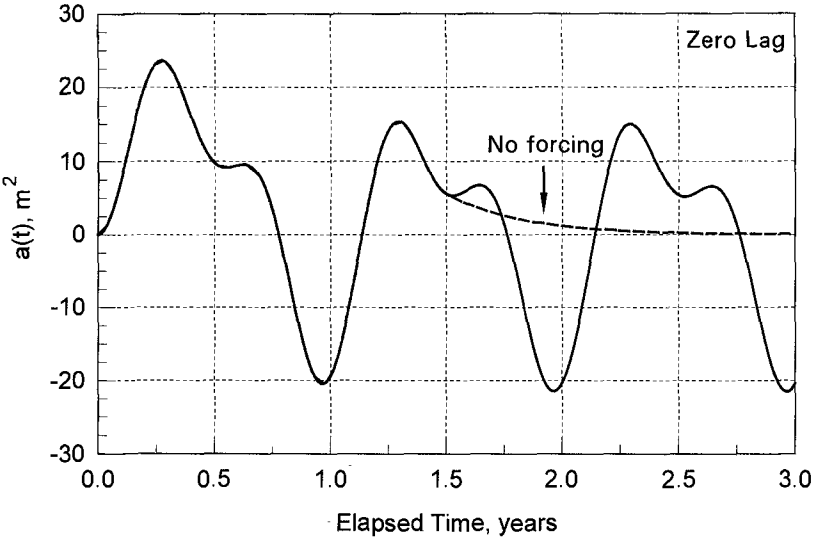

Fig. 4. Change in inlet area around equilibrium for forcing by sinusoidal discharge and sinusoidal longshore sediment transport rate, no lag between the forcings.

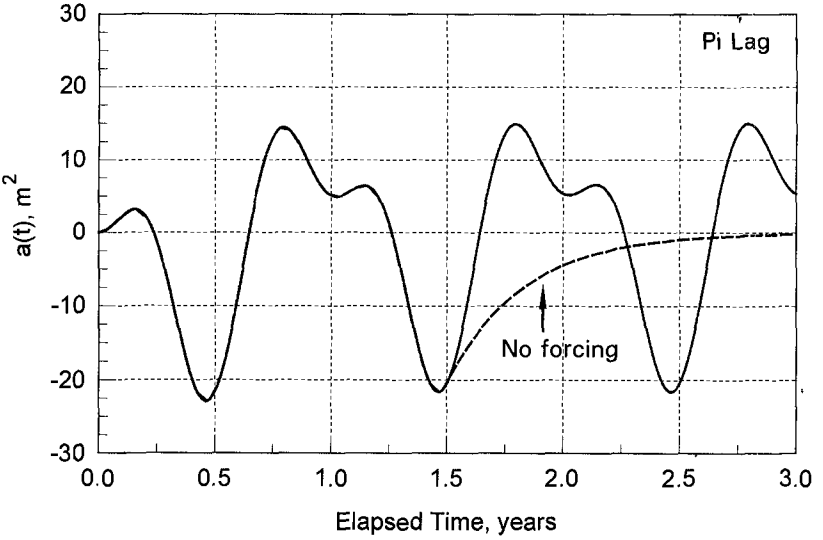

Fig. 5. Change in inlet area around equilibrium for forcing by sinusoidal discharge and sinusoidal longshore sediment transport rate, lag of 180 deg between the forcings.

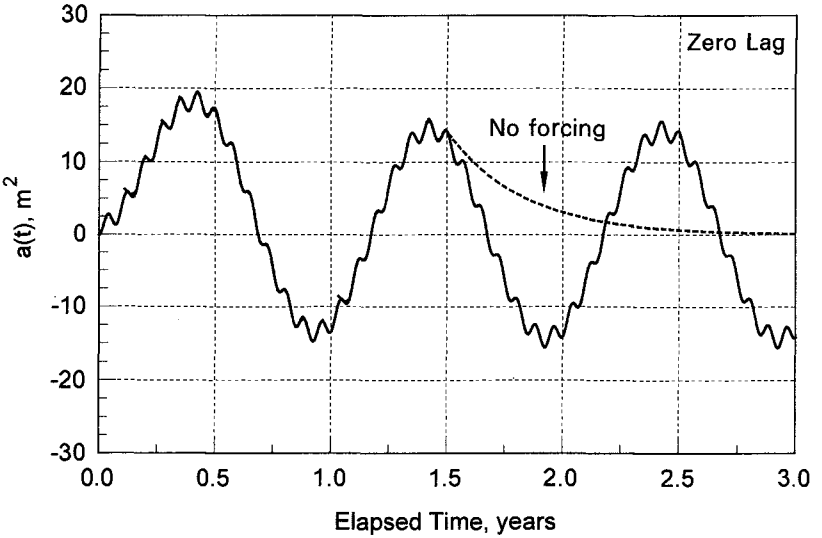

Fig. 6. Change in inlet area around equilibrium for forcing by sinusoidal discharge with rapid (bi-weekly change) and sinusoidal longshore sediment transport rate, no lag between the forcings.

CONCLUDING DISCUSSION

An equation relating the equilibrium or minimum cross-sectional area of an inlet channel was derived by balancing the input of longshore sediment transport with the transporting capacity of the inlet's discharge or tidal prism. The equation has the same functional form as previous empirical equations, but with the empirical coefficient expressed as a function of quantities related to the acting coastal processes. By expressing the inlet discharge in terms of the tidal prism, the derived coefficient C_p was found to have the same order of magnitude as accepted empirical values. The process-based expression qualitatively explains the long-recognized, greater inlet cross-sectional areas, for the same tidal prism, which are observed on more sheltered coasts where longshore sediment transport is less than on exposed coasts.

The time-dependent governing equation was perturbed from equilibrium to give a general linear differential equation describing variations in channel cross-section for small changes in the discharge and longshore sediment transport rate. The equation showed that longer-period perturbations (perturbations with periods comparable to or greater than the relaxation time of the inlet channel) tend to greatly alter the cross-sectional area of an inlet channel.

To arrive at the simple governing equation, three model-defining assumptions were made. First, the channel bar has idealized geometry, by which a simple form of the sediment continuity equation could be derived. Second, sediment exchange such as among the entrance bar, flood shoal, and beaches, is omitted. And third, it was assumed that the sediment-transport dynamics can be represented by relatively simple

expressions. In principle, these assumptions can be weakened or eliminated by extension of the process-based formulation that would be solved numerically. Because little is known about sediment pathways at inlets, a comprehensive process-based model would lend insight to the functioning of these pathways.

In summary, although the model introduced here has limitations, it represents rational incorporation of the main physical processes that have been identified by observations made at coastal tidal inlets by numerous authors. Extensions of the model can readily be accomplished, and the author expects to report some of these in future publications.

POSTSCRIPT

After presentation of this paper at the Twenty-Sixth International Coastal Engineering Conference, an attendee, Dr. Hitoshi Tanaka brought to my attention his work and that of his colleagues at Tohoku University, Japan. Their work concerns river mouth closure, and in it they have introduced a model similar to that of Eq. 4 concerning balance of river discharge and longshore sediment transport. Details can be found in Tanaka et al. (1996), which references an earlier work, Ogawa et al. (1984). Tanaka et al. examine the evolution of the width of an unstabilized river mouth, considering the time dependence of the variable W in the present work.

ACKNOWLEGEMENTS

I appreciate stimulating discussions with Mr. William Seabergh of the U.S. Army Engineer Waterways Experiment Station (WES), Coastal and Hydraulics Laboratory. Also, I would like to thank Dr. Hitoshi Tanaka for providing several articles on his studies related to modeling of river mouth closure that were not available to me. The work reported in this paper was conducted under the Inlet Channels and Adjacent Shorelines Work Unit of the Coastal Inlets Research Program conducted at WES. Permission was granted by Headquarters, U.S. Army Corps of Engineers, to publish this information.

REFERENCES

Behrens, E. W., Watson, R. L., and Mason, C. 1977. Hydraulics and Dynamies of New Corpus Christi Pass, Texas: A Case History, 1972-1973. GITI Report 8, U.S. Army Corps of Engineers, Waterways Experiment Station, Vicksburg, MS.

Bruun, P. 1968. *Tidal Inlets and Littoral Drift*. University Book Co., Oslo, 200 pp.

_____. 1978. *Stability of Tidal Inlets*. Elsevier, New York, 510 pp.

Bruun, P., and Gerritsen, F. 1960. *Stability of Coastal Inlets*. North Holland, Amsterdam, 140 pp.

Byrne, R.J., DeAlteris, J.T., and Bullock, P.S. 1974. Channel Stability in Tidal Inlets: A Case Study. *Proc. 14th Coastal Eng. Conf.*, ASCE Press, NY, 1585-1604.

Byrne, R.J., Gammisch, R.A., and Thomas, G.R. 1980. Tidal Prism-Inlet Area Relations for Small Tidal Inlets. *Proc. 17th Coastal Eng. Conf.*, ASCE Press, NY, 2517-2533.

FitzGerald, D. M. and FitzGerald, S. A. 1977. Factors Influencing Tidal Inlet Geometry. *Proc. Coastal Sediments '77*, ASCE Press, NY, 563-581.

Hume, T.M. and Herdendorf, C. E. 1990. Morphologic and Hydrologic Characteristics of Tidal Inlets on a Headland Dominated, Low Littoral Drift Coast, Northeastern New Zealand, *Proc. Skagen Symposium (2-5 Sep. 199), J. of Coastal Res. Special Issue 9*: 527-563.

Jarrett, J.T. 1976. Tidal Prism-Inlet Area Relationships. GITI. Report 3, U.S. Army Corps of Engineers, Waterways Experiment Station, Vicksburg, MS.

Johnson, J. W. 1972. Tidal Inlets on the California, Oregon, and Washington Coasts. Tech. Rep. HEL 24-12, Hydraulic Engineering Lab., U. of California at Berkeley, Berkeley, CA.

Keulegan, G. H. and Hall, J. V. 1950. A Formula for the Calculation of Tidal Discharge Through an Inlet. U.S. Army Corps of Engineer, Beach Erosion Board Bulletin, Vol. 4, 15-29.

LeConte, L.J. 1905. Discussion on River and Harbor Outlets, "Notes on the Improvement of River and Harbor Outlets in the United States," Paper No. 1009, by D. A. Watts, *Trans., ASCE* 55: 306-308.

Mason, C. and Sorenson, R. M. 1972. Character and Stability of a Natural Tidal Inlet. *Proc. 13th Coastal Eng. Conf.*, ASCE Press, NY, 781-800.

Nummedal, D. and Humphries, S. M. 1978. Hydraulics of North Inlet, South Carolina, 1975-1976. GITI Report 16, U.S. Army Corps of Engineers, Waterways Experiment Station, Vicksburg, MS.

O'Brien, M.P. 1931. Estuary and Tidal Prisms Related to Entrance Areas. *Civil Eng.* 1(8): 738-739.

O'Brien, M.P. 1969. Equilibrium Flow Areas of Inlets on Sandy Coasts. *Jour. Waterways and Harbors Division* 95(WW1): 43-52.

Ogawa, Y., Fujita, Y., and Shuto, N. 1984. Change in the Cross-Sectional Area and Topography of at River Mouth. *Coastal Eng. in Japan*, 27: 233-247.

Riedel, H.P., and Gourlay, M.R. 1980. Inlets/Estuaries Discharging into Sheltered Waters. *Proc. 17th Coastal Eng. Conf.*, ASCE Press, NY, 2550-2562.

Tanaka, H., Takahashi, R., and Takahashi, A. 1996. Complete Closure of the Nanakita River Mouth in 1994. *Proc. 26th Coastal Eng. Conf.*, ASCE Press, NY, 4545-4556.

Van de Kreeke, J. and Haring, J. 1980. Stability of Estuary Mouths in the Rhine-Meuse Delta. *Proc. 18th Coastal Eng. Conf.*, ASCE Press, NY, 2627-2639.

Watanabe, A., Shimuzu, T., and Kondo, K. 1991. Field Application of a Numerical Model of Beach Topography Response. *Proc. Coastal Sediments '91*, ASCE Press, NY, 1814-1928.